Research Square

Preprints are preliminary reports that have not undergone peer review.
They should not be considered conclusive, used to inform clinical practice,
or referenced by the media as validated information.

Fast implementation of controlled π phase gate using superadiabatic shortcuts with Rydberg superatoms

Ruobing Zhao
Bohai University
Wei Li
liweizhd@126.com
Bohai University
Yanqiang Ji
Bohai University
Jie Wang
Bohai University
Shubo Jiang
Bohai University
Xiaoming Xiu
Bohai University

Research Article

Keywords: Superadiabatic shortcuts, Rydberg superatoms, Phase gates, Quantum Zeno dynamics

Posted Date: August 14th, 2026

DOI: https://doi.org/10.21203/rs.3.rs-10073925/v1

License: This work is licensed under a Creative Commons Attribution 4.0 International License.
Read Full License

Additional Declarations: No competing interests reported.

Version of Record: A version of this preprint was published at Quantum Information Processing on October 29th, 2026. See the published version at https://doi.org/10.1007/s11128-026-05370-3.

Fast implementation of controlled π phase gate using superadiabatic shortcuts with Rydberg superatoms

R.B. Zhao[1], W. Li[1*], Y.Q. Ji[1*], J. Wang[1], S.B. Jiang[1], X.M. Xiu[1]

[1*]College of Physical Science and Technology, Bohai University, , Jinzhou, 121013, Liaoning, China.

*Corresponding author(s). E-mail(s): liweizhd@126.com; jiyanqiang@qymail.bhu.edu.cn;

Abstract

Quantum phase gates serve as core fundamental resources for quantum information processing, and their preparation efficiency and structural stability directly determine the overall performance of quantum computing and quantum communication. The traditional adiabatic preparation method is prone to the influence of decoherence due to its excessive time consumption, while superadiabatic shortcut technology can significantly shorten the evolution time while retaining the advantages of the adiabatic process.In this paper, we propose a scheme for rapidly implementing a quantum phase gate by combining superadiabatic scheme and quantum Zeno dynamics to construct shortcuts to adiabatic passage. We demonstrate the superadiabatic shortcut by using Rydberg superatoms in distant-atom-cavity system. Furthermore, we utilize the controlled $\boldsymbol{\pi}$ phase gate to achieve the preparation of N-particles cluster states. Additionally, the impact of decoherence and operational imperfections are discussed. Numerical simulation demonstrates the proposed scheme has high fidelities and robustness against both cavity leakage and atomic spontaneous emission.

Keywords: Superadiabatic shortcuts, Rydberg superatoms, Phase gates, Quantum Zeno dynamics

1 Introduction

Benefiting from unique quantum properties including superposition and entanglement, quantum computing demonstrates tremendous application potential to outperform classical computing in large-number factorization, quantum simulation, and machine learning, and is regarded as one of the core directions of the next-generation information processing technology[1]. As the basic building blocks of quantum computers, the quality of quantum logic gate preparation directly determines the performance upper limit of quantum computing high-fidelity[2], high-stability, and scalable quantum logic gates are the key prerequisites for realizing practical quantum computation[3, 4]. Since the concept of quantum computing was proposed, researchers have explored implementation schemes of quantum logic gates in various physical systems, including superconducting qubits, ion traps, cavity quantum electrodynamics, and Rydberg atoms[5, 6]. Among them, the cavity QED system has become one of the ideal platforms for preparing high-precision quantum logic gates due to its strong coupling characteristics between qubits and light fields and excellent controllability[7]. For example, the Haroche group achieved high-fidelity preparation of single-qubit gates by manipulating the interaction between cavity fields and atoms, laying a foundation for quantum control in the cavity QED system[8, 9].

In the implementation of quantum computing[10] and quantum information processing tasks, it is crucial to select a reasonable physical system [11].In recent years, Rydberg atoms[12] have attracted extensive research attention and are recognized as one of the most promising candidates for quantum computing implementation and many-body physical simulation, have been gaining growing attention in recent years[13]. Rydberg atoms possess two prominent advantages that make them an optimal quantum system. On one hand, Rydberg atoms[14] have an extremely large electric dipole moment, which can generate strong van der Waals force or dipole-dipole interaction effects[15–19], further inducing the Rydberg blockade effect[20], When a single atom is excited to the Rydberg state, it will suppress the excitation behavior of surrounding atoms. Based on this mechanism, a Rydberg atom ensemble can be equivalent to a superatom, The coupling strength between its ground state and excited state is $\sqrt{n}$ times higher than that of a single atom, which reduces the difficulty of experimental regulation[21, 22]. On the other hand, the energy levels and interactions of Rydberg atoms can be precisely regulated through parameters such as laser frequency and intensity, providing a flexible and controllable physical carrier for the construction of quantum logic gates and entangled states[23, 24]. Their energy levels and interaction behaviors can be accurately regulated via proper excitation and control methodologies[25]. Specifically, Researchers can accurately manipulate the excitation and de-excitation processes of Rydberg atoms as well as interatomic interaction behaviors by optimizing excitation modes and laser control parameters.

In recent years, to address the inherent limitation of adiabatic methods, shortcuts to adiabaticity(STA)[26] have emerged as a suite of fast-adiabatic strategies designed to accelerate adiabatic passage[27]. Particularly promising for quantum information processing, STA actively mitigates the adverse effects of decoherence, noise, and losses that accumulate over prolonged operational times[28–32]. Nowadays, STA is a type of technology that simulates the results of adiabatic evolution by designing non-adiabatic

driving fields, the techniques commonly achieve accelerated dynamics by introducing a counterdiabatic driving (CDD) term, which explicitly cancels non-adiabatic transitions, thus circumventing the slow evolution necessitated by the strict adiabatic condition [33]. Numerous proposals have successfully employed STA for various tasks, including rapid population transfer[34], quantum phase gate implementation [35, 36], and entanglement generation [37]. Superadiabatic iteration provides a practical route to realize these techniques, as initially adapted for two-level systems by Ibáñez et al.[38], and later extended to multi-level systems, such as the three-level transitionless quantum driving scheme proposed by Song et al.[39], and it can accurately control quantum systems in a shorter time. Subsequently, Liang et al.formulated a generalized approach to universal quantum gates via superadiabatic shortcuts, exemplified in a nitrogen-vacancy center system[40]. This has spurred further theoretical developments in fast population transfer [41, 42], quantum phase gates [43–47], and entanglement generation[48].

Inspired by previous schemes, this paper leverages a superadiabatic approach to construct shortcuts to adiabatic passage, enabling the rapid implementation of a controlled π phase gate in a system of Rydberg superatoms[49]. The high fidelity and decoherence resistance of the scheme are verified through numerical simulationsand then the rapid preparation of N-particle cluster states is completed through the cascaded operation of phase gates.

This paper is organized as follows. In section 2, we present the physical model of Rydberg superatoms and establish the effective Hamiltonian based on the intrinsic characteristics of the constituent atoms.Then in section 3, we construct shortcuts to adiabatic passage in a system of two spatially separated Rydberg superatoms by virtue of superadiabatic techniques, and further realize a controlled π phase gate. Numerical simulations and discussions regarding the validity of the superadiabatic scheme tailored for Rydberg superatom systems are present in section 4. Subsequently,in Section 5, we exploit the controlled π phase gate to generate N-particles cluster states within N distant cavities that are interconnected via $N-1$ optical fibers. Finally, the conclusion is provided in Section 6.

2 Physical model and effective Hamiltonian

The four-level system of cold 87Rb atoms are depicted in Fig 1(a), with the ground states $|g\rangle \equiv |5\mathrm{S}_{1/2}, F=2, m_F=2\rangle$ and $|m\rangle \equiv |5\mathrm{S}_{1/2}, F=1, m_F=1\rangle$, the excited state $|e\rangle \equiv |5\mathrm{P}_{3/2}, F=3, m_F=3\rangle$ and the Rydberg state $|r\rangle \equiv |60\mathrm{S}_{1/2}, m_J=1/2\rangle$, Specifically,$|g\rangle \leftrightarrow |e\rangle$ transition is coupled to the left circularly polarized mode of the quantized cavity field with a coupling strength of λ,the atomic transitions $|e\rangle$ and $|r\rangle$ are driven by the classical field with a Rabi frequency Ω_a; the atomic transitions $|m\rangle$ and $|e\rangle$ are resonantly driven through a time-dependent laser pulse with Ω_b. V_{vdw} denotes the van der Waals interaction between two atoms in the Rydberg state, which can substantially modify the Rydberg energy levels of adjacent atoms, thus leading to the Rydberg blockade effect[48]. Under this effect, the ensemble functions as an equivalent Rydberg superatom, whose simplified energy-level structure is depicted in Fig 1 (b). Under the rotating-wave approximation, the Hamiltonian of the system in

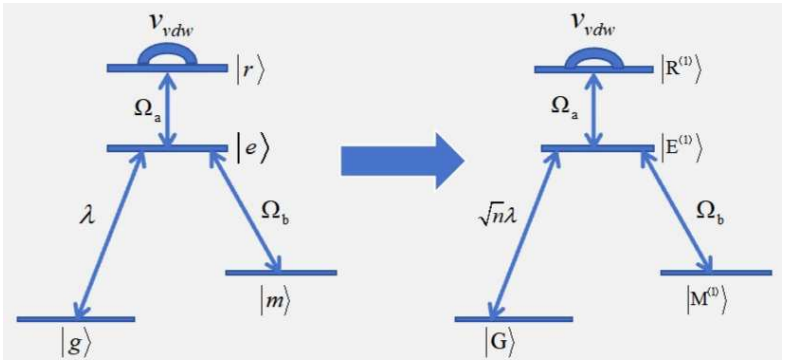


Fig. 1 (a) Rydberg atom energy level configuration; (b) Effective energy level configuration of the superatom when the cavity field is in the weak limit.

the interaction picture takes the form ($\hbar = 1$)

$$H = \sum_k \lambda_k |g\rangle_k\langle e| a_k^\dagger + \Omega_{b,k}|m\rangle_k\langle e| + \Omega_{a,k}|e\rangle_k\langle r| + \text{H.c.} + \sum_{k,j(j>k)} V_{\text{vdw}}|rr\rangle_{kj}\langle rr|. \quad (1)$$

However, owing to the Rydberg blockade effect, only one atom within the superatom can be excited to the Rydberg state $|r\rangle$. Thus, this superatom can be characterized by four collective states $|G\rangle$, $|M^{(1)}\rangle$, $|E^{(1)}\rangle$, and $|R^{(1)}\rangle$, as illustrated in Fig.1(b). These states are defined as follows

$$\begin{aligned}
|G\rangle &= |g_1 g_2 \cdots g_n\rangle, \\
|M^{(1)}\rangle &= \sum_{j=1}^{n} |g_1 g_2 \cdots m_j \cdots g_n\rangle/\sqrt{n}, \\
|E^{(1)}\rangle &= \sum_{j=1}^{n} |g_1 g_2 \cdots e_j \cdots g_n\rangle/\sqrt{n}, \\
|R^{(1)}\rangle &= \sum_{j=1}^{n} |g_1 g_2 \cdots r_j \cdots g_n\rangle/\sqrt{n},
\end{aligned}$$

where n denotes the number of Rydberg atoms. In order to implement two-qubit controlled π phase gate, we consider that two four-level Rydberg superatoms respectively trapped in two cavities connected by a fiber as shown in Fig. 2. So in the interaction picture the Hamiltonian of the system in the interaction picture can be written as

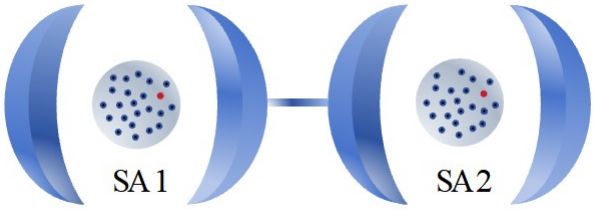


Fig. 2 The cavity-fiber-atom combined system

$$
\begin{aligned}
H_a &= H_l + H_c + H_f, \\
H_l &= \sum_{k=1,2} \Omega_{a,k} |E^{(1)}\rangle_k \langle R^{(1)}| + \sum_{k=1,2} \Omega_{b,k} |M^{(1)}\rangle_k \langle E^{(1)}| + \text{H.c.}, \\
H_c &= \sum_{k=1,2} \sqrt{n_k} \lambda_k |G\rangle \langle E^{(1)}| a_k^\dagger + \text{H.c.}, \\
H_f &= v b^\dagger (a_1 + a_2) + \text{H.c.},
\end{aligned} \tag{2}
$$

where H_c denotes the interaction between the cavity and the superatom, H_l represents the interaction between the classical field and the superatom, and H_f stands for the interaction between the cavity and the optical fiber. $a_k^\dagger$ and a_k is the creation operator and the annihilation operator for photons in the k-th cavity, v denotes the coupling strength between the optical fiber and the cavity, and $b_k^\dagger$and b_k are the operators for the kth optical fiber. n_k and λ_k represent the number of Rydberg atoms and the coupling strength between the Rydberg atoms and the cavity within the k-th superatom, respectively.For the simplicity, we suppose that $\lambda_1 = \lambda_2 = \lambda$.

First, we turn off the classical laser field $\Omega_{b,k}$ (for $k = 1, 2$), when the initial state of the system is $|R^{(1)}\rangle_1 |G\rangle_2 |0\rangle_{c_1} |0\rangle_f |0\rangle_{c_2}$ and then the entire system will evolve within the subspace:

$$
\begin{aligned}
|\alpha_1\rangle &= |R^{(1)}\rangle |G\rangle |0\rangle_1 |0\rangle_f |0\rangle_2, \\
|\alpha_2\rangle &= |E^{(1)}\rangle |G\rangle |0\rangle_1 |0\rangle_f |0\rangle_2, \\
|\alpha_3\rangle &= |G\rangle |G\rangle |1\rangle_1 |0\rangle_f |0\rangle_2, \\
|\alpha_4\rangle &= |G\rangle |G\rangle |0\rangle_1 |1\rangle_f |0\rangle_2, \\
|\alpha_5\rangle &= |G\rangle |G\rangle |0\rangle_1 |0\rangle_f |1\rangle_2, \\
|\alpha_6\rangle &= |G\rangle |E^{(1)}\rangle |0\rangle_1 |0\rangle_f |0\rangle_2, \\
|\alpha_7\rangle &= |G\rangle |R^{(1)}\rangle |0\rangle_1 |0\rangle_f |0\rangle_2.
\end{aligned} \tag{3}
$$

By employing the basis vectors from Eq.(3), the Hamiltonian of the system in the interaction picture in the interaction picture can be rewritten as

$$\begin{aligned}
&H'_a = H'_c + H'_f + H'_l,\\
&H'_{cl} = H'_c + H'_l,\\
&H'_c = \sqrt{n}\lambda|\alpha_2\rangle\langle\alpha_3| + \sqrt{n}\lambda|\alpha_6\rangle\langle\alpha_5| + \text{H.c.},\\
&H'_l = \Omega_{a,1}|\alpha_2\rangle\langle\alpha_1| + \Omega_{a,2}|\alpha_6\rangle\langle\alpha_7| + \text{H.c.},\\
&H'_f = v|\alpha_3\rangle\langle\alpha_4| + v|\alpha_4\rangle\langle\alpha_5| + \text{H.c.}.
\end{aligned} \tag{4}$$

Under the Zeno condition $\sqrt{n}\lambda_k \gg \Omega'_{a,k}$, the Hilbert subspace is split into five invariant Zeno subspaces

$$Z_1 = \{\langle\alpha_1|, |\beta_0\rangle, \langle\alpha_7|\}, \quad Z_2 = \{|\beta_1\rangle\}, \quad Z_3 = \{|\beta_2\rangle\}, \quad Z_4 = \{|\beta_3\rangle\}, \quad Z_5 = \{|\beta_4\rangle\}, \tag{5}$$

corresponding to the projections $P_i = \sum_{m\in Z_i} |m\rangle\langle m|$, with the corresponding eigenvalues

$$\nu_0 = 0, \quad \nu_1 = \sqrt{n}\lambda, \quad \nu_2 = -\sqrt{n}\lambda, \quad \nu_3 = \chi, \quad \nu_4 = -\chi, \tag{6}$$

where the states

$$\begin{aligned}
|\beta_0\rangle &= \frac{v}{\chi}(|\alpha_2\rangle - \frac{\sqrt{n}\lambda}{v}|\alpha_4\rangle + |\alpha_6\rangle),\\
|\beta_1\rangle &= \frac{1}{2}(-|\alpha_2\rangle - |\alpha_3\rangle + |\alpha_5\rangle + |\alpha_6\rangle),\\
|\beta_2\rangle &= \frac{1}{2}(-|\alpha_2\rangle + |\alpha_3\rangle - |\alpha_5\rangle + |\alpha_6\rangle),\\
|\beta_3\rangle &= \frac{\sqrt{n}\lambda}{2\chi}(|\alpha_2\rangle + \frac{\chi}{\sqrt{n}\lambda}|\alpha_3\rangle + \frac{2v}{\sqrt{n}\lambda}|\alpha_4\rangle + \frac{\chi}{\sqrt{n}\lambda}|\alpha_5\rangle + |\alpha_6\rangle),\\
|\beta_4\rangle &= \frac{\sqrt{n}\lambda}{2\chi}(|\alpha_2\rangle - \frac{\chi}{\sqrt{n}\lambda}|\alpha_3\rangle + \frac{2v}{\sqrt{n}\lambda}|\alpha_4\rangle - \frac{\chi}{\sqrt{n}\lambda}|\alpha_5\rangle + |\varphi_6\rangle),
\end{aligned} \tag{7}$$

are eigenstates of H_c. Through performing the unitary transformation $U = \exp(-i\sum \nu_n|\beta_n\rangle\langle\beta_n|t)$ and neglecting the terms with high oscillating, we obtain the effective Hamiltonian($\chi = \sqrt{2\nu^2 + \lambda^2}$)

$$\begin{aligned}
H_{\text{eff}} &= \frac{v}{\chi}|\beta_0\rangle\left(\Omega_{a,1}\langle\alpha_1| + \Omega_{b,2}\langle\alpha_7|\right) + \text{H.c.}\\
&= \frac{v}{\chi}\begin{pmatrix} 0 & \Omega_{a,1}(t) & 0\\ \Omega_{a,1}(t) & 0 & \Omega_{b,2}(t)\\ 0 & \Omega_{b,2}(t) & 0 \end{pmatrix}
\end{aligned} \tag{8}$$

where $\Omega_1 = v\Omega_{a,1}/\chi$ and $\Omega_2 = v\Omega_{b,1}/\chi$. For convenience, let $|\alpha_1\rangle = (100)^{\text{T}}$, $|\beta_0\rangle = (010)^{\text{T}}$, and $|\alpha_7\rangle = (001)^{\text{T}}$. So the effective Hamiltonian can be rewritten as

$$H_{eff} = \Omega(t) \begin{pmatrix} 0 & \sin\theta_1(t) & 0 \\ \sin\theta_1(t) & 0 & \cos\theta_1(t) \\ 0 & \cos\theta_1(t) & 0 \end{pmatrix} \tag{9}$$

where $\theta_1(t) = \arctan\Omega_1(t)/\Omega_2(t)$, $\Omega(t) = \sqrt{\Omega_1^2(t) + \Omega_2^2(t)}$. The eigenvalues of this effective Hamiltonian are $\zeta_0 = 0$ and $\zeta_\pm = \pm\Omega(t)$, and the corresponding eigenstates are $|\varphi_0(t)\rangle = \begin{pmatrix} \cos\theta_1(t) \\ 0 \\ -\sin\theta_1(t) \end{pmatrix}$, $|\varphi_\pm(t)\rangle = \frac{1}{\sqrt{2}} \begin{pmatrix} \sin\theta_1(t) \\ \pm 1 \\ \cos\theta_1(t) \end{pmatrix}$.

3 Superadiabatic shortcuts for two qubit controlled π phase gate

According to the superadiabatic evolution theory[50, 51], we convert the effective Hamiltonian to the adiabatic frame using the adiabatic basis $|\psi_{0,\pm}(t)\rangle$, this is done via the unitary transformation $A_0(t) = \sum_{i=0,\pm} |\psi_i\rangle\langle\psi_i(t)|$[52]. We perform a unitary transformation on the Hamiltonian: By expanding the outer product $|\psi_k\rangle\langle\psi_k(t)|$ and summing them up, the matrix form of $A_0(t)$ is:

$$A_0(t) = \begin{pmatrix} \cos\theta_1(t) & \frac{\sin\theta_1(t)}{\sqrt{2}} & \frac{\sin\theta_1(t)}{\sqrt{2}} \\ 0 & \frac{1}{\sqrt{2}} & -\frac{1}{\sqrt{2}} \\ -\sin\theta_1(t) & \frac{\cos\theta_1(t)}{\sqrt{2}} & \frac{\cos\theta_1(t)}{\sqrt{2}} \end{pmatrix}, \tag{10}$$

So the Hamiltonian becomes

$$\begin{aligned} H_1(t) &= A_0(t) H_{\text{eff}}(t) A_0^\dagger(t) - i A_0(t) \dot{A}_0^\dagger(t) \\ &= \frac{1}{\sqrt{2}} \begin{pmatrix} -\sqrt{2}\Omega(t) & i\dot{\theta}(t) & 0 \\ -i\dot{\theta}(t) & 0 & -i\dot{\theta}(t) \\ 0 & i\dot{\theta}(t) & \sqrt{2}\Omega(t) \end{pmatrix}. \end{aligned} \tag{11}$$

Within the adiabatic approximation framework, a system evolves along the adiabatic states $|\psi_{0,\pm}(t)\rangle$ when the corresponding adiabatic condition $|\Omega(t)| \gg |\dot{\theta}_1(t)/\sqrt{2}|$ is satisfied, this criterion ensures that the inter-eigenstate coupling strength (quantified by terms like $|\dot{\theta}_1(t)/\sqrt{2}|$) remains negligible. However, slow variations of Hamiltonian parameters (required to meet this condition) lead to a protracted evolution process, while rapid parameter adjustments induce unwanted transitions between distinct eigenstates, creating a trade-off between evolution speed and state purity. To resolve this trade-off (accelerating the system dynamics while suppressing inter-eigenstate transitions of the effective Hamiltonian H_{eff}) researchers proposed the counterdiabatic driving (CDD)[53] strategy: modifying the original time-dependent H_{eff} with a tailored CDD Hamiltonian. It precisely cancels the coupling-inducing term $-i\dot{A}_0(t)A_0^\dagger(t)$in the

Hamiltonian, thereby effectively suppressing unintended eigenstate transitions.

$$\begin{aligned} H_{CD}^{(1)}(t) &= i\dot{A}_0^{\dagger}(t)A_0(t) \\ &= i\dot{\theta}(t)(|\alpha_7\rangle\langle\alpha_1| - |\alpha_1\rangle\langle\alpha_7|) \\ &= \begin{pmatrix} 0 & 0 & i\dot{\theta}(t) \\ 0 & 0 & 0 \\ -i\dot{\theta}(t) & 0 & 0 \end{pmatrix}. \end{aligned} \tag{12}$$

However, Eq.(15) indicates that the counterdiabatic Hamiltonian to be added needs to couple directly to $|\alpha_1\rangle$ and $|\alpha_7\rangle$, which is generally challenging to implement in practical operations. To find a feasible Hamiltonian, we analyze the system by entering the superadiabatic picture (i.e., performing a second picture iteration). The Hamiltonian $H_1(t))$ with the basis$|\varphi_{0,+,-}\rangle$ corresponding to the eigenvalues $\eta_0 = 0$ and $\eta_{\pm} = \pm\Omega'(t)$, where $\Omega'(t)$ is defined as $\Omega'(t) = \sqrt{\Omega^2(t) + \dot{\theta}_1^2(t)}$. The corresponding eigenstates are

$$|\xi_0(t)\rangle = -i\sin\theta_2(t)|\psi_0\rangle - \frac{\cos\theta_2(t)}{\sqrt{2}}|\psi_+\rangle + \frac{\cos\theta_2(t)}{\sqrt{2}}|\psi_-\rangle \tag{13}$$

$$|\xi_+(t)\rangle = \frac{1}{\sqrt{2}}\left[-i\frac{\cos\theta_2(t)}{\sqrt{2}}|\psi_0\rangle + \frac{1}{2}\left(1+\sin\theta_2(t)\right)|\psi_+\rangle + \frac{1}{2}\left(1-\sin\theta_2(t)\right)|\psi_-\rangle\right] \tag{14}$$

$$|\xi_-(t)\rangle = \frac{1}{\sqrt{2}}\left[-i\frac{\cos\theta_2(t)}{\sqrt{2}}|\psi_0\rangle + \frac{1}{2}\left(1-\sin\theta_2(t)\right)|\psi_+\rangle + \frac{1}{2}\left(1+\sin\theta_2(t)\right)|\psi_-\rangle\right] \tag{15}$$

we transform $H_1(t)$ into the superadiabatic framework, by proceeding with the second unitary transformation. So in the superadiabatic framework, Hamiltonian can be written by

$$\begin{aligned} H_2(t) &= A_1(t)H_1(t)A_1^{\dagger}(t) - iA_1(t)\dot{A}_1^{\dagger}(t) \\ &= \frac{1}{\sqrt{2}}\begin{pmatrix} -\sqrt{2}\Omega'(t) & i\dot{\theta}_1(t) & 0 \\ -i\dot{\theta}_1(t) & 0 & -i\dot{\theta}_1(t) \\ 0 & i\dot{\theta}_1(t) & \sqrt{2}\Omega'(t) \end{pmatrix}. \end{aligned} \tag{16}$$

We use$|\ \beta_0\rangle$, $|\ \alpha_7\rangle$ and $|\ \alpha_1\rangle$ as the basis vectors, the new counterdiabatic Hamiltonian can be written by

$$\begin{aligned} H_{CD}^{(2)}(t) &= iA_0^{+}(t)\dot{A}_1^{+}(t)A_1(t)A_0(t) \\ &= \dot{\theta}_1(t)\left(-\cos\theta_0(t)\mid\beta_0\rangle\langle\alpha_1\mid + \sin\theta_0(t)\mid\beta_0\rangle\langle\alpha_7\mid\right) + \text{H.c.} \\ &= \dot{\theta}_1(t)\begin{pmatrix} 0 & \cos\theta(t) & 0 \\ \cos\theta(t) & 0 & \sin\theta(t) \\ 0 & \sin\theta(t) & 0 \end{pmatrix}. \end{aligned} \tag{17}$$

To evolve the initial state $|R^{(1)}\rangle_1|G\rangle_2\,|0\rangle_{c_1}\,|0\rangle_{c_2}\,|0\rangle_f$ to the target state $-|R^{(1)}\rangle_1|G\rangle_2\,|0\rangle_{c_1}\,|0\rangle_{c_2}\,|0\rangle_f$, the parameters should satisfy the boundary conditions:

$\theta_2(0) = \theta_2(t) = 0, \theta_1(0) = -\pi/2, \theta_1(t) = \pi/2$, then the effective Hamiltonian with the addition of the correction term is

$$\begin{aligned} H_{\rm d}(t) &= H_{\rm eff}(t) + H_{CD}^{(2)}(t) \\ &= \Omega_u^a(t)|\beta_0\rangle\langle\alpha_1| + \Omega_u^b(t)|\beta_0\rangle\langle\alpha_7| + \text{H.c.} \end{aligned} \tag{18}$$

If the initial state of the system is $|R^{(1)}\rangle_1|M^{(1)}\rangle_2|0\rangle_{c_1}|0\rangle_f|0\rangle_{c_2}$, the whole system will evolve in the subspace spanned by

$$\begin{array}{lll}
|R^{(1)}\rangle_1|M^{(1)}\rangle_2|0\rangle_{c_1}|0\rangle_f|0\rangle_{c_2}, & |E^{(1)}\rangle_1|M^{(1)}\rangle_2|0\rangle_{c_1}|0\rangle_f|0\rangle_{c_2}, & |G\rangle_1|M^{(1)}\rangle_2|1\rangle_{c_1}|0\rangle_f|0\rangle_{c_2}, \\
|M^{(1)}\rangle_1|M^{(1)}\rangle_2|0\rangle_{c_1}|0\rangle_f|0\rangle_{c_2}, & |E^{(1)}\rangle_1|G\rangle_2|0\rangle_{c_1}|0\rangle_f|1\rangle_{c_2}, & |G\rangle_1|M^{(1)}\rangle_2|0\rangle_{c_1}|1\rangle_f|0\rangle_{c_2}, \\
|G\rangle_1|R^{(1)}\rangle_2|0\rangle_{c_1}|1\rangle_f|0\rangle_{c_2}, & |G\rangle_1|M^{(1)}\rangle_2|0\rangle_{c_1}|0\rangle_f|1\rangle_{c_2}, & |G\rangle_1|E^{(1)}\rangle_2|1\rangle_{c_1}|0\rangle_f|0\rangle_{c_2}, \\
|G\rangle_1|E^{(1)}\rangle_2|0\rangle_{c_1}|0\rangle_f|1\rangle_{c_2}, & |G\rangle_1|G\rangle_2|1\rangle_{c_1}|0\rangle_f|1\rangle_{c_2}, & |G\rangle_1|R^{(1)}\rangle_2|0\rangle_{c_1}|0\rangle_f|1\rangle_{c_2}, \\
|G\rangle_1|G\rangle_2|1\rangle_{c_1}|1\rangle_f|0\rangle_{c_2}, & |G\rangle_1|G\rangle_2|0\rangle_{c_1}|1\rangle_f|1\rangle_{c_2}, & |G\rangle_1|G\rangle_2|2\rangle_{c_1}|0\rangle_f|0\rangle_{c_2}, \\
|G\rangle_1|G\rangle_2|0\rangle_{c_1}|0\rangle_f|2\rangle_{c_2}, & |G\rangle_1|G\rangle_2|0\rangle_{c_1}|2\rangle_f|0\rangle_{c_2}, & |G\rangle_1|(E^{(1)}R^{(1)})\rangle_2|0\rangle_{c_1}|0\rangle_f|0\rangle_{c_2}, \\
|E^{(2)}\rangle_1|G\rangle_2|0\rangle_{c_1}|0\rangle_f|0\rangle_{c_2}, & |G\rangle_1|E^{(2)}\rangle_2|0\rangle_{c_1}|0\rangle_f|0\rangle_{c_2}, & |G\rangle_1|(E^{(1)}M^{(1)})\rangle_2|0\rangle_{c_1}|0\rangle_f|0\rangle_{c_2}, \\
|R^{(1)}\rangle_1|R^{(1)}\rangle_2|0\rangle_{c_1}|0\rangle_f|0\rangle_{c_2}, & |R^{(1)}\rangle_1|E^{(1)}\rangle_2|0\rangle_{c_1}|0\rangle_f|0\rangle_{c_2}, & |(E^{(1)}M^{(1)})\rangle_1|G\rangle_2|0\rangle_{c_1}|0\rangle_f|0\rangle_{c_2}, \\
|E^{(1)}\rangle_1|R^{(1)}\rangle_2|0\rangle_{c_1}|0\rangle_f|0\rangle_{c_2}, & |R^{(1)}\rangle_1|G\rangle_2|0\rangle_{c_1}|0\rangle_f|1\rangle_{c_2}, & |(E^{(1)}R^{(1)})\rangle_1|G\rangle_2|0\rangle_{c_1}|0\rangle_f|0\rangle_{c_2}, \\
|M^{(1)}\rangle_1|R^{(1)}\rangle_2|0\rangle_{c_1}|0\rangle_f|0\rangle_{c_2}, & |M^{(1)}\rangle_1|E^{(1)}\rangle_2|0\rangle_{c_1}|0\rangle_f|0\rangle_{c_2}, & |M^{(1)}\rangle_1|G\rangle_2|0\rangle_{c_1}|0\rangle_f|1\rangle_{c_2}, \\
|E^{(1)}\rangle_1|E^{(1)}\rangle_2|0\rangle_{c_1}|0\rangle_f|0\rangle_{c_2}, & &
\end{array} \tag{19}$$

where $(R^{(1)}M^{(1)})$ denotes that one Rydberg atom is in $|R^{(1)}\rangle$ state, one Rydberg atom is in $|M^{(1)}\rangle$ state, and the residual Rydberg atoms are in $|G\rangle$ state. Following a procedure analogous to that of Eqs. (4) to (9), the effective Hamiltonian simplifies to 0.

$$H_{eff}|R^{(1)}\rangle_1|M^{(1)}\rangle_2|0\rangle_{c_1}|0\rangle_f|0\rangle_{c_2} = 0, \tag{20}$$

And under the Zeno condition $\Omega_{a,1} \ll \lambda$, v, neglecting the high-frequency oscillating terms, we can obtain the final effective Hamiltonian $H_{\rm eff} = 0$. So, the evolution is forbidden when the initial state of system is $|R^{(1)}\rangle_1|M^{(1)}\rangle_2|0\rangle_{c_1}|0\rangle_{c_2}|0\rangle_f$ Clearly, the total Hamiltonian has no effect on the evolution of the initial states $|G\rangle_1|M^{(1)}\rangle_2|0\rangle_{c_1}|0\rangle_{c_2}|0\rangle_f$ and $|G\rangle_1|G\rangle_2|0\rangle_{c_1}|0\rangle_{c_2}|0\rangle_f$,

$$\begin{aligned} H_{eff}|G\rangle_1|M^{(1)}\rangle_2|0\rangle_{c_1}|0\rangle_f|0\rangle_{c_2} = 0, \\ H_{eff}|G\rangle_1|G\rangle_2|0\rangle_{c_1}|0\rangle_f|0\rangle_{c_2} = 0, . \end{aligned} \tag{21}$$

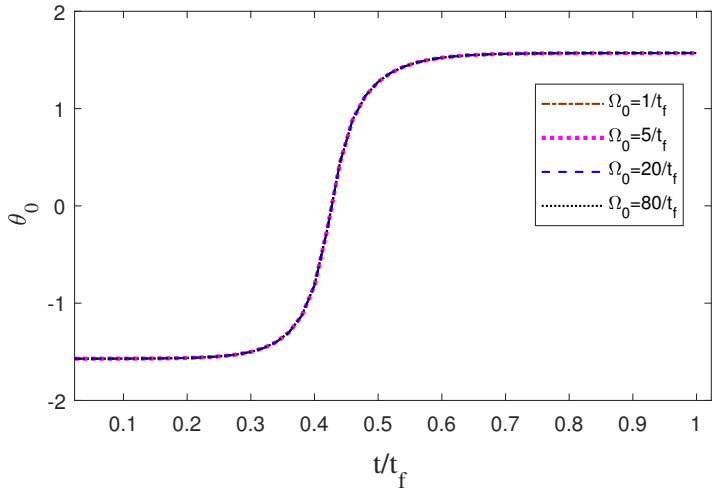


Fig. 3 θ_0 vs t/t_f with different pulse amplitude.

Therefore, it can be concluded that

$$\begin{aligned}
&|R^{(1)}\rangle_1|M^{(1)}\rangle_2|0\rangle_{c_1}|0\rangle_f|0\rangle_{c_2} \rightarrow |R^{(1)}\rangle_1|M^{(1)}\rangle_2|0\rangle_{c_1}|0\rangle_f|0\rangle_{c_2},\\
&|G\rangle_1|G\rangle_2|0\rangle_{c_1}|0\rangle_f|0\rangle_{c_2} \rightarrow |G\rangle_1|G\rangle_2|0\rangle_{c_1}|0\rangle_f|0\rangle_{c_2},\\
&|G\rangle_1|M^{(1)}\rangle_2|0\rangle_{c_1}|0\rangle_f|0\rangle_{c_2} \rightarrow |G\rangle_1|M^{(1)}\rangle_2|0\rangle_{c_1}|0\rangle_f|0\rangle_{c_2},\\
&|R^{(1)}\rangle_1|G\rangle_2|0\rangle_{c_1}|0\rangle_f|0\rangle_{c_2} \rightarrow -|R^{(1)}\rangle_1|G\rangle_2|0\rangle_{c_1}|0\rangle_f|0\rangle_{c_2}.
\end{aligned} \tag{22}$$

which is a two qubit controlled π phase gate.

4 Numerical simulation and discussion

First, we select Gaussian pulses $\Omega_m(t)$ and $\Omega_n(t)$ based on reference[54].

$$\begin{aligned}
\Omega_m(t) = &-20\Omega_0 \exp\left[-(t-\tau_{11})^2/T^2\right] + 10\Omega_0 \exp\left[-(t-\tau_{12})^2/T^2\right]\\
&- 0.1\,\Omega_0 \exp\left[-(t-\tau_{13})^2/T^2\right],\\
\Omega_n(t) = &\,0.3\Omega_0 \exp\left[-(t-\tau_{21})^2/T^2\right],
\end{aligned} \tag{23}$$

Where Ω_0 represents the amplitude of the driving pulse, t_f denotes the total evolution time of the pulse sequence. The time delays of the pulses are defined as $\tau_{11} = 0.01t_f$, $\tau_{12} = 0.8t_f$, $\tau_{13} = 0.6t_f$ and $\tau_{21} = 0.45t_f$, with the pulse width set to $T = 0.2t_f$. Based on these parameters, the time-dependent driving pulses $\Omega_m(t)$ and $\Omega_n(t)$ can be utilized to derive the time-varying angular functions $\theta_0(t)$ and $\theta_1(t)$. As depicted in

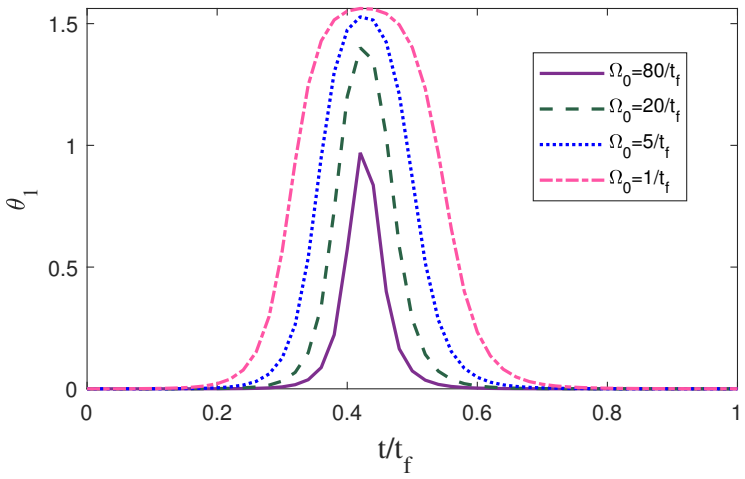


Fig. 4 θ_1 vs t/t_f with different pulse amplitude.

Fig.3 and Fig.4, the variations of $\theta_0(t)$ and $\theta_1(t)$ with the normalized evolution time are illustrated, which characterizes the dynamic behavior of the driving pulse.

As illustrated in Fig.3, the angular function $\theta_0(t)$ consistently satisfies the boundary conditions $\theta_0(t) = -\pi/2$ regardless of the driving pulse amplitude Ω_0 (the curves for $\Omega_0 = 1/t_f$, $\Omega_0 = 5/t_f$, $\Omega_0 = 20/t_f$ and $\Omega_0 = 80/t_f$ are fully overlapping). For the parameter $\theta_1(t)$ (shown in Fig.4), increasing Ω_0 causes its boundary values to approach 0 more closely; however, the conditions $\theta_1(0) = \theta_1(t) = 0$ are only fulfilled when Ω_0 is sufficiently large. Note that within this work, the constraints $\Omega_k(t) \ll \lambda, v(k = 1, 2, 3)$ must be maintained, so Ω_0 cannot be excessively large. Thus, we select $\Omega_0 = 0.5/t_f, \lambda = 80/t_f$ for subsequent analyses.

To validate the performance of the proposed scheme, Fig.5 illustrates the functional dependence of the target state's fidelity on time. Throughout the entire evolution process, when the time exceeds $0.8t/t_f$, the fidelity gradually stabilizes; the final fidelity value is 0.992. This indicates that the scheme is feasible and effective for implementing a high-fidelity controlled π phase gate. It can be concluded that the scheme proposed in this paper is feasible and effective, enabling the preparation of controlled π phase gates with high fidelity. However, the effective Hamiltonian of the system is obtained by neglecting high-frequency oscillatory terms during picture transformation. In addition, during the parameter control process, the target quantum state of the system may evolve into other extraneous quantum states in the course of quantum evolution. Consequently, the final fidelity cannot reach unity.

Fig.6 presents the population dynamics of all quantum states throughout the entire evolution process, which demonstrates that a high-fidelity controlled π phase gate can be achieved following the system's evolution. From the figure, it is evident that

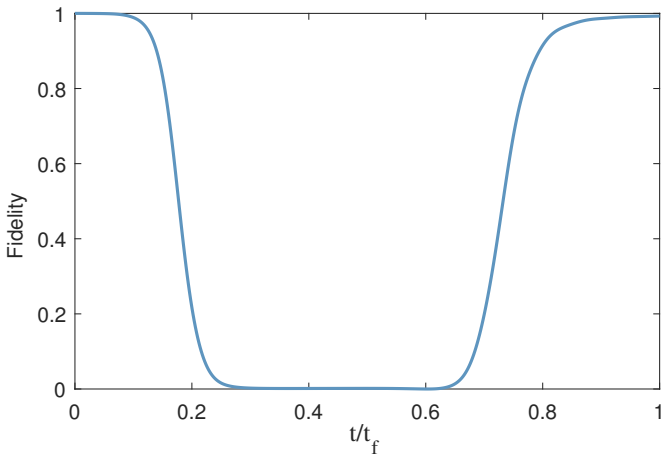


Fig. 5 Fidelity of the target state F as a function of t/t_f.

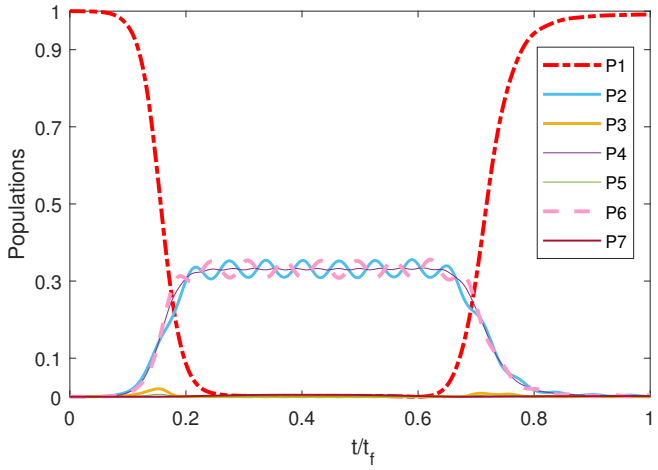


Fig. 6 Time evolution of the populations for the states.

all states stabilize once the normalized time exceeds $0.9t/t_f$. The intermediate states $|\alpha_2\rangle$, $|\alpha_4\rangle$ and $|\alpha_6\rangle$ only emerge within the time window $0.1t/t_f$ and $0.9t/t_f$, with their population values remaining below 0.4. Notably, the population of state $|\alpha_3\rangle$, $|\alpha_5\rangle$ and $|\alpha_7\rangle$ remains nearly zero across the entire evolution. Thus, in the proposed scheme, the decoherence effects caused by photon leakages can be neglected.

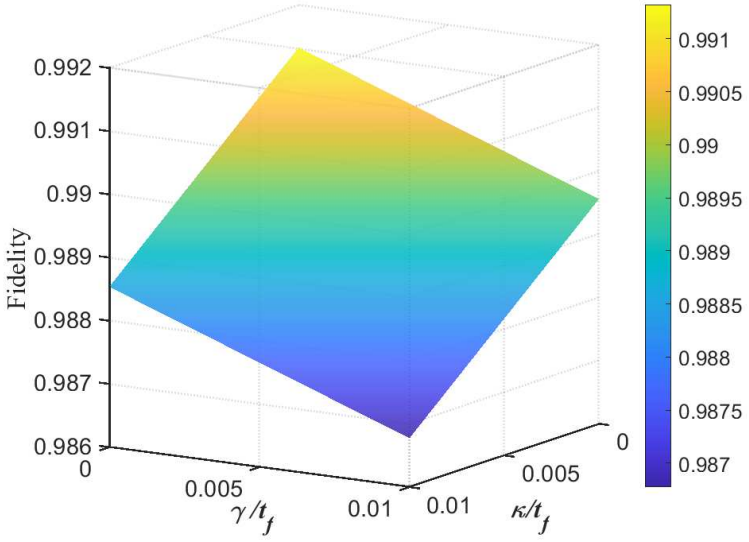


Fig. 7 The fidelity F of the target state$-|\alpha_1\rangle$ versus the γt_f, κt_f.

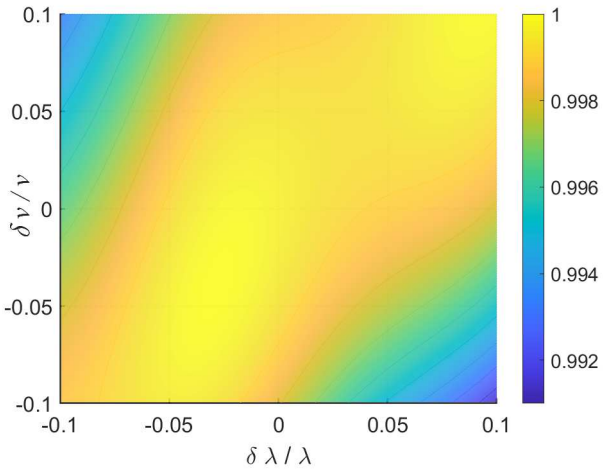


Fig. 8 The fidelity F versus the λ and v.

Finally, we investigate the robustness of the scheme against decoherence induced by atomic spontaneous emission, cavity decay and fiber decay from the cavity fiber system. The evolution of the system can be described by the following master equation

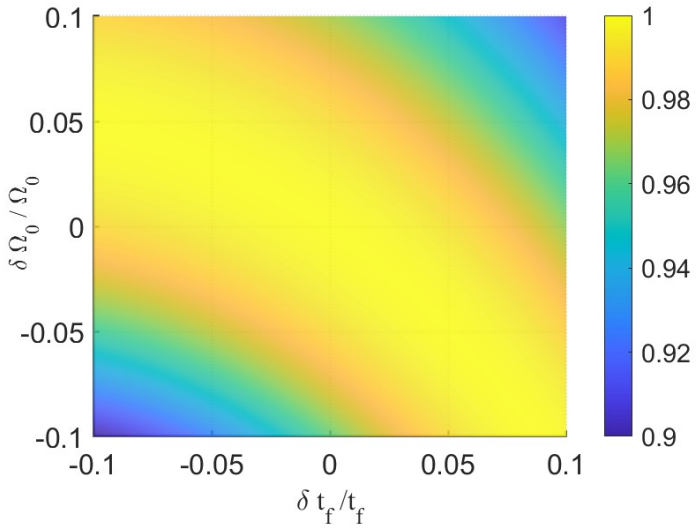


Fig. 9 The fidelity F versus the Ω_0 and t_f.

$$\dot{\rho} = i[\rho, H_a] + \sum_k [L_k \rho L_k^\dagger - \frac{1}{2}(L_k^\dagger L_k \rho + \rho L_k^\dagger L_k)], \tag{24}$$

where ρ is the density operator for the whole system, and L_k are the so-called Lindblad operators. We consider the initial state $|\alpha_1\rangle$. For the implementation of the controlled π phase gate, there are seven Lindblad operators that govern dissipation in the model:

$$\begin{aligned} &L_1 = \sqrt{\gamma_1}|E^{(1)}\rangle_1\langle R^{(1)}|,\ L_2 = \sqrt{\gamma_2}|E^{(1)}\rangle_2\langle R^{(1)}|, \\ &L_3 = \sqrt{\gamma_3}|G\rangle_1\langle E^{(1)}|,\ L_4 = \sqrt{\gamma_4}|G\rangle_2\langle E^{(1)}|, \\ &L_5 = \sqrt{\kappa_1}a_1,\ L_6 = \sqrt{\kappa_2}a_2,\ L_7^{\kappa_f} = \sqrt{\kappa_f}b, \end{aligned} \tag{25}$$

where $\gamma_n (n = 1, 2, \cdots, 4)$ are the atomic spontaneous emissions, $\kappa_j\,(j = 1, 2)$ are the cavity decays, and κ_f is the fiber decay. For simplicity, we set $\gamma_i = \gamma/2$ and $\kappa_j = \kappa_f = \kappa$. In Fig.7, we plot the fidelity F_1 of the target state $-|\alpha_1\rangle$ through the relation $F = |\langle -\alpha_1|\rho(t_f)| - \alpha_1\rangle|$ versus the dimensionless parameters γt_f and κt_f via numerically solving the master equation in Eq.(24). In Fig.7, the superadiabatic scheme exhibits remarkable robustness against decoherence induced by both atomic spontaneous emissions and cavity decay from the cavity-fiber system, because even when $\kappa t_f = \gamma t_f = 0.01$, the final fidelity can keep very high, i.e., $F > 0.985$.Thus, the controlled π phase gate exhibits robustness against both decay and decoherence.

Since operational deviations are inevitably incurred in practical operation processes, we further investigated the influence of fluctuations in the parameter λ and the

fiber-cavity coupling strength v on the final fidelity. In Fig.8 presents the relationship between the final fidelity and the relative errors of these parameters, and it can be seen from the results that the proposed scheme exhibits excellent robustness against fluctuations in the parameters λ and v. In Fig.9 presents the relationship between the fidelity and the pulse with the t_f, and it can be seen from the results that the proposed scheme exhibits excellent robustness.

5 Preparation of cluster states

Here, we describe how cluster states can be prepared using the controlled π phase gate. As depicted in Fig.10, N Rydberg superatoms (SA_1 through SA_N) are trapped within N cavities (c_1, c_2, ..., c_N), which are linked via $N-1$ optical fibers (f_1, f_2, ..., f_{N-1}) paired with corresponding optical switches (O_1, O_2, ..., O_{N-1}). To prevent unintended interactions between the superatoms at the outset, all optical switches are kept in the off state initially. We turn on the optical switch O_1: this allows the associated fiber to mediate coupling between cavities c_1 and c_2. Following this setup, we initialize SA_1 and SA_2 into the quantum state

$$\begin{aligned}|C_1\rangle &= \frac{1}{2}(|R^{(1)}\rangle_1 + |G\rangle_1)(|M^{(1)}\rangle_2 + |G\rangle_2) \\ &= \frac{1}{2}(|R^{(1)}\rangle_1|M^{(1)}\rangle_2 + |R^{(1)}\rangle_1|G\rangle_2 + |G\rangle_1|M^{(1)}\rangle_2 + |G\rangle_1|G\rangle_2). \end{aligned} \tag{26}$$

Using the two qubit controlled π phase gate achieved above in section 3, we easily obtain a two-particle cluster state as follows

$$\begin{aligned}|C_1^{'}\rangle &= \frac{1}{2}(|R^{(1)}\rangle_1|M^{(1)}\rangle_2 - |R^{(1)}\rangle_1|G\rangle_2 + |G\rangle_1|M^{(1)}\rangle_2 + |G\rangle_1|G\rangle_2) \\ &= \frac{1}{2}(|R^{(1)}\rangle_1\sigma_2^z + |G\rangle_1)(|M^{(1)}\rangle_2 + |G\rangle_2), \end{aligned} \tag{27}$$

where $\sigma_2^z = |M^{(1)}\rangle_2\langle M^{(1)}| - |G\rangle_2\langle G|$. Then, the optical switch O_1 is turned off, and O_2 is turned on. Meanwhile, atom 3 is prepared in the state $(|R^{(1)}\rangle_3 + |G\rangle_3)/\sqrt{2}$. In this situation, the entire system is

$$\begin{aligned}|C_2\rangle &= \frac{1}{2}(|R^{(1)}\rangle_1\sigma_2^z + |G\rangle_1)(|M^{(1)}\rangle_2 + |G\rangle_2) \otimes \frac{1}{\sqrt{2}}(|R^{(1)}\rangle_3 + |G\rangle_3) \\ &= \frac{1}{\sqrt{2}}(|R^{(1)}\rangle_1\sigma_2^z + |G\rangle_1)\frac{1}{2}(|M^{(1)}\rangle_2|R^{(1)}\rangle_3 + |M^{(1)}\rangle_2|G\rangle_3 + |G\rangle_2|R^{(1)}\rangle_3 + |G\rangle_2|G\rangle_3). \end{aligned} \tag{28}$$

Subsequently, we turn off the laser pulses $\Omega_{a,k}$ (with $k = 2, 3$ and switch on the laser pulses $\Omega_{b,k}$ (illustrated in Fig. 1(b)). Following the same calculation approach as in the preceding section, we can derive another controlled π phase gate, which induces the following state transformations

$$|G\rangle_2|R^{(1)}\rangle_3|0\rangle_{c_2}|0\rangle_{c_3}|0\rangle_{f_2} \rightarrow |G\rangle_2|R^{(1)}\rangle_3|0\rangle_{c_2}|0\rangle_{c_3}|0\rangle_{f_2},$$

$$
\begin{aligned}
&|G\rangle_2|G\rangle_3|0\rangle_{c_2}|0\rangle_{c_3}|0\rangle_{f_2} \rightarrow |G\rangle_2|G\rangle_3|0\rangle_{c_2}|0\rangle_{c_3}|0\rangle_{f_2},\\
&|M^{(1)}\rangle_2|R^{(1)}\rangle_3|0\rangle_{c_2}|0\rangle_{c_3}|0\rangle_{f_2} \rightarrow |M^{(1)}\rangle_2|R^{(1)}\rangle_3|0\rangle_{c_2}|0\rangle_{c_3}|0\rangle_{f_2},\\
&|M^{(1)}\rangle_2|G\rangle_3|0\rangle_{c_2}|0\rangle_{c_3}|0\rangle_{f_2} \rightarrow -|M^{(1)}\rangle_2|G\rangle_3|0\rangle_{c_2}|0\rangle_{c_3}|0\rangle_{f_2}. \qquad (29)
\end{aligned}
$$

A three-particle cluster state is obtained by applying this phase gate to the state $|C_2\rangle$

$$
\begin{aligned}
|C_2^{'}\rangle &= \frac{1}{\sqrt{2}}(|R^{(1)}\rangle_1\sigma_2^z + |G\rangle_1)\frac{1}{2}(|M^{(1)}\rangle_2|R^{(1)}\rangle_3 - |M^{(1)}\rangle_2|G\rangle_3 + |G\rangle_2|R^{(1)}\rangle_3 + |G\rangle_2|G\rangle_3)\\
&= \frac{1}{2\sqrt{2}}((|R^{(1)}\rangle_1\sigma_2^z + |G\rangle_1)(|M^{(1)}\rangle_2\sigma_3^z + |G\rangle_2)(|R^{(1)}\rangle_3 + |G\rangle_3), \qquad (30)
\end{aligned}
$$

where $\sigma_3^z = |R^{(1)}\rangle_3\langle R^{(1)}| - |G\rangle_3\langle G|$. By analogy, once an $(N-1)$ particle cluster state has been created, it is easy to generate an N-particle cluster state using the above procedures.

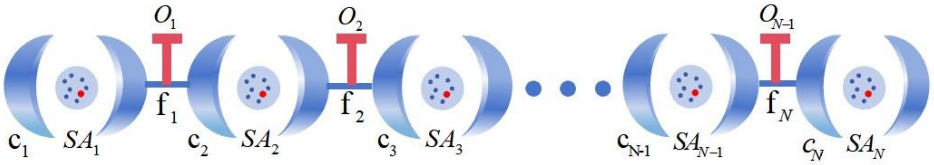


Fig. 10 The setup diagram for the creation of cluster states.

In the experiment, the ^{87}Rb atomic ensemble can be placed in a magneto-optical trap (MOT) within an ultra-high vacuum cavity to prepare Rydberg superatoms[55]. And cesium atoms also serve as viable candidates for implementing the proposed schemes. By employing fiber-taper coupling to high-Q silica microspheres[56], an almost ideal fiber-cavity coupling efficiency exceeding 99.9% can be achieved. For an 852-nm wavelength, the fiber loss is measured to be merely approximately 2.2 dB per kilometer, corresponding to a fiber decay rate of just 0.152 MHz. Moreover, recent experimental studies predict that a strong atom-cavity coupling strength of $\lambda = 2\pi \times 750$ MHz can be attained under such conditions. This implies that the fiber decay rate is effectively negligible in actual experiments utilizing these parameters[57, 58]. Additionally, when an alternative set of parameters $(\lambda, \Gamma, \kappa) = (2500, 10, 10)$ MHz—reported in microsphere cavity quantum electrodynamics (QED) studies is adopted, the fidelity of the π phase gate exceeds 99% [59, 60].

6 Conclusion

In this paper, we propose a scheme for the rapid preparation of a two qubit controlled π phase gate basing Ryberg superatoms via the superadiabatic shortcut method. As an application example, we prepare multi-particle cluster states by using the controlled π phase gate. Numerical simulation results confirm the efficient preparation performance of this two-qubit controlled π phase gate. Further analysis of the effects

of spontaneous emission and decoherence shows that the final fidelity can still be maintained at 0.991, demonstrating that the controlled π phase gate prepared by this scheme exhibits excellent robustness and stability. As the second iterative picture, the superadiabatic scheme is more complicated but much more easily achieved in experiment. Additionally, the coupling strength between ground state and excited state of superatoms can be enhanced by a factor of $\sqrt{n}$ compared with an individual Rydberg atom, so the experimental requirements are reduced. Therefore, our scheme might be a more reliable choice in experiment.

Acknowledgements

This work was supported by the Joint Program of Liaoning Provincial Science and Technology Plan (Key Research and Development Program) (Grant No. 2025JH2/101800128), the Education Administration program of Liaoning Province (Grant Nos. LJ212410167045), the Key Programs of Bohai University (Grant No. 0525xn071), the General Programs of Bohai University (Grant No. 0525xn078).

Declarations

The authors declare no conflict of interest.
The data that support the findings of this study are available from the corresponding author upon reasonable request.

References

[1] Itano, W.M., Heinzen, D.J., Bollinger, J.J., Wineland, D.J.: Quantum zeno effect. Physical Review A **41**(5), 2295 (1990)

[2] Duan, L.-M., Wang, B., Kimble, H.: Robust quantum gates on neutral atoms with cavity-assisted photon scattering. Physical Review A **72**(3), 032333 (2005)

[3] Facchi, P., Pascazio, S.: Quantum zeno subspaces. Physical review letters **89**(8), 080401 (2002)

[4] Sleator, T., Weinfurter, H.: Realizable universal quantum logic gates. Physical Review Letters **74**(20), 4087 (1995)

[5] DiVincenzo, D.P.: Two-bit gates are universal for quantum computation. Physical Review A **51**(2), 1015 (1995)

[6] Neeley, M., Bialczak, R.C., Lenander, M., Lucero, E., Mariantoni, M., O'connell, A., Sank, D., Wang, H., Weides, M., Wenner, J., *et al.*: Generation of three-qubit entangled states using superconducting phase qubits. Nature **467**(7315), 570–573 (2010)

[7] Haljan, P.C., Brickman, K.-A., Deslauriers, L., Lee, P.J., Monroe, C.: Spin-dependent forces on trapped ions for phase-stable quantum gates and entangled states of spin and motion. Physical review letters **94**(15), 153602 (2005)

[8] Lo, H.-P., Ikuta, T., Matsuda, N., Honjo, T., Takesue, H.: Entanglement generation using a controlled-phase gate for time-bin qubits. Applied Physics Express **11**(9), 092801 (2018)

[9] Fu, Z., Xu, P., Sun, Y., Liu, Y.-Y., He, X.-D., Li, X., Liu, M., Li, R.-B., Wang, J., Liu, L., *et al.*: High-fidelity entanglement of neutral atoms via a rydberg-mediated single-modulated-pulse controlled-phase gate. Physical Review A **105**(4), 042430 (2022)

[10] Saffman, M., Walker, T.G., Mølmer, K.: Quantum information with rydberg atoms. Reviews of modern physics **82**(3), 2313 (2010)

[11] Omran, A., Levine, H., Keesling, A., Semeghini, G., Wang, T.T., Ebadi, S., Bernien, H., Zibrov, A.S., Pichler, H., Choi, S., *et al.*: Generation and manipulation of schrodinger cat states in rydberg atom arrays. Science **365**(6453), 570–574 (2019)

[12] Paris-Mandoki, A., Braun, C., Kumlin, J., Tresp, C., Mirgorodskiy, I., Christaller, F., Büchler, H.P., Hofferberth, S.: Free-space quantum electrodynamics with a single rydberg superatom. Physical Review X **7**(4), 041010 (2017)

[13] Su, S.-L., Li, W.: Dipole-dipole-interaction–driven antiblockade of two rydberg atoms. Physical Review A **104**(3), 033716 (2021)

[14] Urban, E., Johnson, T.A., Henage, T., Isenhower, L., Yavuz, D., Walker, T., Saffman, M.: Observation of rydberg blockade between two atoms. Nature Physics **5**(2), 110–114 (2009)

[15] Shao, X.-Q., Su, S.-L., Li, L., Nath, R., Wu, J.-H., Li, W.: Rydberg superatoms: An artificial quantum system for quantum information processing and quantum optics. Applied Physics Reviews **11**(3) (2024)

[16] Urban, E., Johnson, T.A., Henage, T., Isenhower, L., Yavuz, D., Walker, T., Saffman, M.: Observation of rydberg blockade between two atoms. Nature Physics **5**(2), 110–114 (2009)

[17] Zhang, W.-Y., Wang, C.-Q., Ji, Y.-Q., Shao, Q.-P., Wang, J.-P., Wang, J., Yang, L.-P., Dong, L., Xiu, X.-M.: Fast preparation of w states by designing the evolution operators with rydberg superatom. Advanced Quantum Technologies **7**(1), 2300140 (2024)

[18] Shao, X., Li, D., Ji, Y., Wu, J., Yi, X.: Ground-state blockade of rydberg atoms and application in entanglement generation. Physical Review A **96**(1), 012328

(2017)

[19] Su, S.-L., Li, W.: Dipole-dipole-interaction–driven antiblockade of two rydberg atoms. Physical Review A **104**(3), 033716 (2021)

[20] Su, S.-L.: Rydberg quantum controlled-phase gate with one control and multiple target qubits. Chinese Physics B **27**(11), 401–407 (2018)

[21] Su, S.-L., Liang, E., Zhang, S., Wen, J.-J., Sun, L.-L., Jin, Z., Zhu, A.-D.: One-step implementation of the rydberg-rydberg-interaction gate. Physical Review A **93**(1), 012306 (2016)

[22] Shao, X., Liu, F., Xue, X., Mu, W., Li, W.: High-fidelity interconversion between greenberger-horne-zeilinger and w states through floquet-lindblad engineering in rydberg atom arrays. Physical Review Applied **20**(1), 014014 (2023)

[23] Su, S.-L., Liang, E., Zhang, S., Wen, J.-J., Sun, L.-L., Jin, Z., Zhu, A.-D.: One-step implementation of the rydberg-rydberg-interaction gate. Physical Review A **93**(1), 012306 (2016)

[24] Su, S.-L., Shao, X.-Q., Wang, H.-F., Zhang, S.: Scheme for entanglement generation in an atom-cavity system via dissipation. Physical Review A **90**(5), 054302 (2014)

[25] Song, X.-K., Ai, Q., Qiu, J., Deng, F.-G.: Physically feasible three-level transitionless quantum driving with multiple schrödinger dynamics. Physical Review A **93**(5), 052324 (2016)

[26] Omran, A., Levine, H., Keesling, A., Semeghini, G., Wang, T.T., Ebadi, S., Bernien, H., Zibrov, A.S., Pichler, H., Choi, S., *et al.*: Generation and manipulation of schrodinger cat states in rydberg atom arrays. Science **365**(6453), 570–574 (2019)

[27] Su, S.-L., Gao, Y., Liang, E., Zhang, S.: Fast rydberg antiblockade regime and its applications in quantum logic gates. Physical Review A **95**(2), 022319 (2017)

[28] Shao, X., Liu, F., Xue, X., Mu, W., Li, W.: High-fidelity interconversion between greenberger-horne-zeilinger and w states through floquet-lindblad engineering in rydberg atom arrays. Physical Review Applied **20**(1), 014014 (2023)

[29] Su, S.-L., Sun, L.-N., Liu, B.-J., Yan, L.-L., Yung, M.-H., Li, W., Feng, M.: Rabi-and blockade-error-resilient all-geometric rydberg quantum gates. Physical Review Applied **19**(4), 044007 (2023)

[30] Chen, X., Torrontegui, E., Muga, J.G.: Lewis-riesenfeld invariants and transitionless quantum driving. Physical Review A **83**(6), 062116 (2011)

[31] Su, S.-L., Guo, F.-Q., Tian, L., Zhu, X.-Y., Yan, L.-L., Liang, E.-J., Feng, M.:

Nondestructive rydberg parity meter and its applications. Physical Review A **101**(1), 012347 (2020)

[32] Shao, X., Wu, J., Yi, X., Long, G.-L.: Dissipative preparation of steady greenberger-horne-zeilinger states for rydberg atoms with quantum zeno dynamics. Physical Review A **96**(6), 062315 (2017)

[33] Su, S.-L., Li, W.: Dipole-dipole-interaction–driven antiblockade of two rydberg atoms. Physical Review A **104**(3), 033716 (2021)

[34] Shao, X., Li, D., Ji, Y., Wu, J., Yi, X.: Ground-state blockade of rydberg atoms and application in entanglement generation. Physical Review A **96**(1), 012328 (2017)

[35] Sun, H.-W., Wu, J.-L., Su, S.-L.: Floquet geometric entangling gates in ground-state manifolds of rydberg atoms. arXiv preprint arXiv:2405.00471 (2024)

[36] Song, P.-Y., Wei, J.-F., Xu, P., Yan, L.-L., Feng, M., Su, S.-L., Chen, G.: Fast realization of high-fidelity nonadiabatic holonomic quantum gates with a time-optimal-control technique in rydberg atoms. Physical Review A **109**(2), 022613 (2024)

[37] Raussendorf, R., Browne, D.E., Briegel, H.J.: Measurement-based quantum computation on cluster states. Physical review A **68**(2), 022312 (2003)

[38] Shao, X.-Q., Su, S.-L., Li, L., Nath, R., Wu, J.-H., Li, W.: Rydberg superatoms: An artificial quantum system for quantum information processing and quantum optics. Applied Physics Reviews **11**(3) (2024)

[39] Löw, R., Weimer, H., Nipper, J., Balewski, J.B., Butscher, B., Büchler, H.P., Pfau, T.: An experimental and theoretical guide to strongly interacting rydberg gases. Journal of Physics B: Atomic, Molecular and Optical Physics **45**(11), 113001 (2012)

[40] Gaëtan, A., Miroshnychenko, Y., Wilk, T., Chotia, A., Viteau, M., Comparat, D., Pillet, P., Browaeys, A., Grangier, P.: Observation of collective excitation of two individual atoms in the rydberg blockade regime. Nature Physics **5**(2), 115–118 (2009)

[41] Colombe, Y., Steinmetz, T., Dubois, G., Linke, F., Hunger, D., Reichel, J.: Strong atom–field coupling for bose–einstein condensates in an optical cavity on a chip. Nature **450**(7167), 272–276 (2007)

[42] Pritchard, J.D., Maxwell, D., Gauguet, A., Weatherill, K.J., Jones, M., Adams, C.S.: Cooperative atom-light interaction in a blockaded rydberg ensemble. Physical review letters **105**(19), 193603 (2010)

[43] Lukin, M.D., Fleischhauer, M., Cote, R., Duan, L., Jaksch, D., Cirac, J.I., Zoller, P.: Dipole blockade and quantum information processing in mesoscopic atomic ensembles. Physical review letters **87**(3), 037901 (2001)

[44] Beterov, I., Saffman, M., Yakshina, E., Tretyakov, D., Entin, V., Hamzina, G., Ryabtsev, I.: Simulated quantum process tomography of quantum gates with rydberg superatoms. Journal of Physics B: Atomic, Molecular and Optical Physics **49**(11), 114007 (2016)

[45] Paris-Mandoki, A., Braun, C., Kumlin, J., Tresp, C., Mirgorodskiy, I., Christaller, F., Büchler, H.P., Hofferberth, S.: Free-space quantum electrodynamics with a single rydberg superatom. Physical Review X **7**(4), 041010 (2017)

[46] Scully, M.O., Fry, E.S., Ooi, C.R., Wódkiewicz, K.: Directed spontaneous emission from an extended ensemble of n atoms: Timing is everything. Physical review letters **96**(1), 010501 (2006)

[47] Liu, Y.-L., Ji, Y.-Q., Han, X., Cui, W.-X., Zhang, S., Wang, H.-F.: Fast conversion of three-particle dicke states to four-particle dicke states with rydberg superatoms. Advanced Quantum Technologies **6**(4), 2200173 (2023)

[48] Yan, D., Cui, C.-L., Liu, Y.-M., Song, L.-J., Wu, J.-H.: Normal and abnormal nonlinear electromagnetically induced transparency due to dipole blockade of rydberg excitation. Physical Review A **87**(2), 023827 (2013)

[49] Su, S.-L., Wang, C., Song, P.-Y., Chen, G.: Nonadiabatic holonomic quantum computation based on rydberg ground state blockade. Chinese Physics Letters **41**(04), 30–36 (2024)

[50] Zeiher, J., Schauß, P., Hild, S., Macrì, T., Bloch, I., Gross, C.: Microscopic characterization of scalable coherent rydberg superatoms. Physical Review X **5**(3), 031015 (2015)

[51] Zhang, W.-Y., Wang, C.-Q., Ji, Y.-Q., Shao, Q.-P., Wang, J.-P., Wang, J., Yang, L.-P., Dong, L., Xiu, X.-M.: Fast preparation of w states by designing the evolution operators with rydberg superatom. Advanced Quantum Technologies **7**(1), 2300140 (2024)

[52] Wang, C., Ji, Y., Zhang, W., Wang, J., Zhang, Z., Liu, Y., Dong, L., Xiu, X.: Fast preparation of dicke state by shortcuts to adiabatic passages. Results in Physics **63**, 107868 (2024)

[53] Shao, X.-Q., Su, S.-L., Li, L., Nath, R., Wu, J.-H., Li, W.: Rydberg superatoms: An artificial quantum system for quantum information processing and quantum optics. Applied Physics Reviews **11**(3) (2024)

[54] Xuemei, W., Anqi, Z., Shengmei, Z.: Realization of controlled-phase gates based

on super-adiabatic shortcuts in circuit quantum electrodynamics. Acta Physica Sinica **71**(15), 7–15 (2022)

[55] Shao, X.Q., Wang, Z.H., Liu, H.D., Yi, X.X.: Dissipative preparation of a tripartite singlet state in coupled arrays of cavities via quantum feedback control. Physical Review A **94**(3), 032307 (2016)

[56] Su, S.-L., Shao, X.-Q., Wang, H.-F., Zhang, S.: Scheme for entanglement generation in an atom-cavity system via dissipation. Physical Review A **90**(5), 054302 (2014)

[57] Giannelli, L., Arimondo, E.: Three-level superadiabatic quantum driving. Physical Review A **89**(3), 033419 (2014)

[58] Saffman, M., Walker, T.G., M?lmer, K.: Quantum information with rydberg atoms. Reviews of Modern Physics **82**(3), 2313–2363 (2010)

[59] Demirplak, M., Rice, S.A.: Adiabatic population transfer with control fields. J. Phys. Chem. A **107**(46), 9937–9945 (2003)

[60] Facchi, P., Pascazio, S.: Quantum zeno dynamics: mathematical and physical aspects. Journal of Physics A: Mathematical and Theoretical **41**(49), 493001 (2008)